

## Turbulence due to spiral breakup in a continuous excitable medium

M. Bär and M. Eiswirth

*Fritz-Haber-Institut der Max-Planck-Gesellschaft, Faradayweg 4-6, W-1000 Berlin 33, Germany*

(Received 9 June 1993)

Excitable media are extended spatial systems, which support the propagation of waves including pulses and rotating spirals. They are well described by sets of partial differential equations involving a fast activator and a slow inhibitor variable. Here we show that spiral breakup, leading to turbulence, can occur in a two-dimensional reaction-diffusion system with delayed-inhibitor production. Upon a decrease of excitability, spirals become unstable because their wavelengths and periods are too short to be sustained in the system.

PACS number(s): 82.20.—w

A considerable amount of recent experimental and theoretical work in the field of spatiotemporal self-organization in biological, chemical, and physical systems has been dedicated to excitable media [1]. The interest in this topic is motivated by the fact that wave propagation in these media provides an efficient mechanism for communication between distant locations. Seminal examples are the conduction of electrical impulses along nerve axons [2] (respectively, cardiac tissue [3]) and the aggregation of the slime mold *Dictyostelium discoideum* [4]. In two dimensions the formation and behavior of spiral waves have been studied in great detail with the Belousov-Zhabotinsky reaction [5]. Most experimentally found phenomena could be reproduced by numerical simulation of simple two-variable models of partial differential equations (PDE's) [6], although the underlying dynamics of the real system usually involves more degrees of freedom. Herein we are concerned with the transition from rotating spiral waves to turbulent wave patterns in terms of such a simple model and its implications on several experimental findings.

The system investigated is a modified version of a piecewise linearized FitzHugh-Nagumo model [7],

$$\frac{du}{dt} = -\frac{1}{\epsilon} u(u-1) \left[ u - \frac{v+b}{a} \right] + \nabla^2 u, \quad (1a)$$

$$\frac{dv}{dt} = f(u) - v. \quad (1b)$$

Instead of the linear ansatz  $f(u)=u$  from [7], the following function was chosen, which leads to inhibitor production only above a threshold value of  $u$ :

$$f(u) = \begin{cases} 0, & u < \frac{1}{3} \\ 1 - 6.75u(u-1)^2, & \frac{1}{3} \leq u \leq 1 \\ 1, & u > 1. \end{cases} \quad (1c)$$

Such a form of  $f(u)$  has been found for surface reactions such as the CO oxidation of Pt(110), where adsorbate-induced structural changes require a threshold coverage [8].

Actually, spiral breakup has been observed without de-

layed inhibitor production in (discrete) cellular automaton models [9] and in coarsely discretized PDE systems [10]. Neither of these examples gives a hint as to the mechanism of this instability. Furthermore, use of discrete models might lead to numerical artifacts, which vanish in the continuous case. Consequently, sufficiently fine grids (cf. [6]) were used here ( $dx=0.39$ ,  $dt=0.031$  for  $\epsilon > 0.04$ ) and all effects found were checked with finer grids.

The decisive parameters in the present context are  $b$  (which determines the excitation threshold) and  $\epsilon$  [which is the relationship of the time scales of the fast (activator,  $u$ ) and the slow (inhibitor,  $v$ ) variable]. The excitability of a system may be defined by the inverse of  $\epsilon$ . Upon increase of  $\epsilon$  the ability of an excitable media to propagate waves usually is lost [6].

The system of equations (1) exhibits a saddle-node bifurcation at  $b=0$ , which leads to oscillations for negative  $b$ , and is excitable for small positive  $b$  and  $a < 1+b$ . A typical nullcline picture in this region is reproduced in Fig. 1. In addition to the rest state, there are two unstable fixed points. Upon a considerable increase of  $\epsilon$ , a limit cycle is formed around the unstable node in a saddle loop bifurcation, which subsequently vanishes via a Hopf bifurcation, giving rise to bistability. In the excitable region, pulse propagation in one spatial dimension persists to unusually high values of  $\epsilon$  [compared to the standard model with  $f(u)=u$ ] as the pulses wind around the unstable fixed points and the front is stabilized by the delay in the inhibitor production (cf. Fig. 1). With increasing  $\epsilon$  the refractory zone shrinks until eventually reexcitation behind the pulse of activation appears, which leads to emission of a pulse in the opposite site direction (backfiring). This behavior — quite unusual for excitable media — evoked some expectations for the two-dimensional system.

For a broad range of  $b$  ( $b < 0.18$ ,  $a=0.84$ ) the following scenario was found. Starting at  $\epsilon=0.01$  rigidly rotating spirals existed up to  $\epsilon=0.06$ , at which point they started to meander, i.e., the spiral tip moved along a flowerlike curve instead of a simple cycle [6,7,11]. For  $\epsilon > 0.07$ , spirals began to break up after some transient rotations, as illustrated in Fig. 2. The resulting free ends

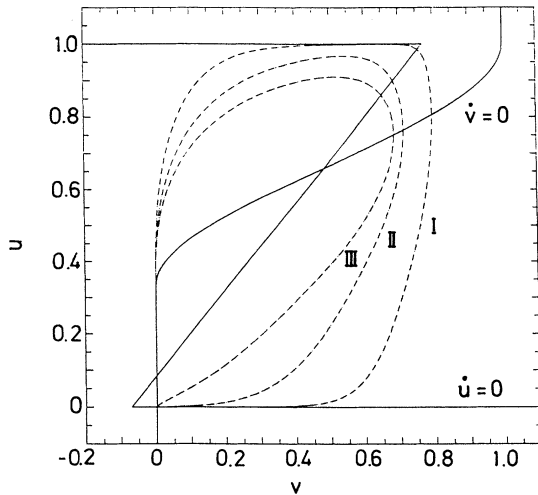


FIG. 1. Nullclines of Eq. (1) with  $a=0.84$ ,  $b=0.07$ . The dashed lines show profiles of solitary pulses for different  $\epsilon$  (I:  $\epsilon=0.04$ ; II:  $\epsilon=0.07$ ; III:  $\epsilon=0.10$ ) indicating a shrinking refractory tail ( $u=0$ ,  $v>0$ ) for increasing  $\epsilon$ .

created new spirals, which in turn broke after some time, eventually giving rise to a noncoherent (turbulent) state (Fig. 2). The spread of the turbulent pattern was considerably slower than the propagation of the outer spiral arms.

This spiral instability can be rationalized as follows: The dispersion relation in excitable media exhibits a minimum temporal period  $\tau_{\min}$ , below which no periodic wave train solutions exist. When  $\epsilon$  is increased, this minimum period allowed by the dispersion relation grows

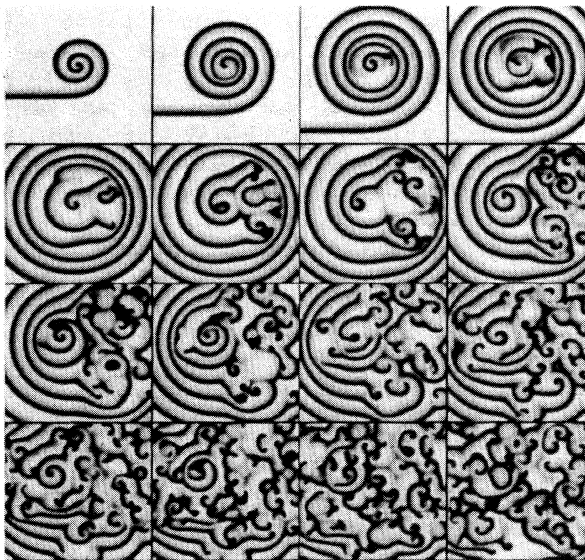


FIG. 2. Development of turbulence at  $a=0.84$ ,  $b=0.07$ ,  $\epsilon=0.08$ . Area of one picture is  $100 \times 100$  (grid points used:  $256 \times 256$ ). Time difference between pictures is 6.41. The initial condition was a flat broken wave. The gray level is proportional to the  $v$  concentration.

faster (with  $\epsilon^\alpha$ ) than the rotation period  $\tau_0$  of the spiral (with  $\epsilon^\beta$ ). The exponent  $\beta$  was derived analytically in the low- $\epsilon$  limit to be  $\frac{1}{3}$  [12]. Numerical simulations [6] yielded approximately  $\frac{1}{2}$  for  $\alpha$  and  $\frac{1}{3}$  for  $\beta$ . Both results were obtained by use of the FitzHugh-Nagumo model. Within the present model these values are  $\alpha=0.6$  and  $\beta=0.4$  (taken from Fig. 3 at  $\epsilon < 0.06$ ). Spirals become unstable if the two values  $\tau_0$  and  $\tau_{\min}$  merge, because the periodic sequence of spiral arms has to fulfill the dispersion relation, i.e.,  $\tau_0 > \tau_{\min}$ . After the onset of meandering, the resulting motion of the spiral core gets faster with growing  $\epsilon$  and consequently a large variation of the period due to the Doppler effect appears in the inner spiral arms (i.e., the meandering tip is regarded as a moving source of periodic waves [13]; Fig. 3). Finally, the smallest period caused by the Doppler effect fell below the minimum period of wave trains in the one-dimensional system (as given by the dispersion relation computed according to [6]). Thus in the propagation direction of the tip, the waves are pressed too close together. Over an arc length of roughly  $\frac{2}{3}\pi$  the inner part of the spiral arm was annihilated (which results in two open ends).

The transition to turbulence vanishes at high excitation threshold  $b$ . In accordance with other systems [6] at higher  $\epsilon$ , first shrinking flat waves were formed, then excitability was lost altogether. The complete phase diagram is reproduced in Fig. 4. Note that there are two separate regions of meandering spirals. The boundary between the turbulent regions T1 and T2 is defined by the onset of backfiring in the one-dimensional system, but is not associated with an abrupt change of the behavior in two dimensions, rather with increasing  $\epsilon$  the trajectories spend on average more time winding around the unstable node and do not reach the stable equilibrium anymore. At the same time the concentration distribution is

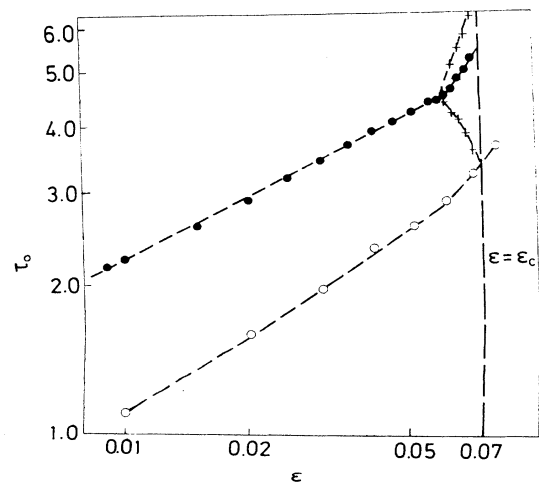


FIG. 3. Spiral rotation period  $\tau_0$  at fixed  $a=0.84$ ,  $b=0.07$  for different values of  $\epsilon$ . After the onset of meandering ( $\epsilon=0.06$ ) the mean period is drawn (full circles), while crosses show the minimum and maximum periods near the spiral center (measured at the point where the breakup first occurs for  $\epsilon=\epsilon_c$ ). Open circles give minimum periods  $\tau_{\min}$  of one-dimensional wave trains.

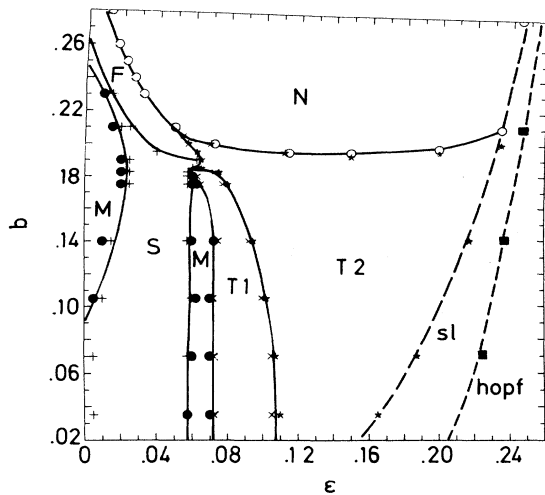


FIG. 4. Phase diagram revealing regions of different wave forms: flat waves (F), spirals with rigid rotation (S), meandering spirals (M), turbulence 1 (T1, cf. Fig. 2), turbulence 2 (T2, backfiring), no waves (N). Dotted lines show bifurcations in the reaction part of Eqs. (1). The saddle loop bifurcation (sl) creates a stable limit cycle around the unstable fixed point. This limit cycle is then destroyed by a Hopf bifurcation (hopf), which changes the unstable fixed point into a stable one. Note that there are two meandering regions in contrast to one in the standard models [6].

smear out. The turbulent patterns in the regions T1 and T2 are phenomenologically very similar to the defect-mediated turbulence in the complex Ginzburg-Landau equation [14], which describes, however, a medium exhibiting smooth oscillations, in contrast to the present excitable model, where the homogeneous rest

state coexists with the turbulence.

We presented calculations with the piecewise linear system (1). It should be mentioned that the phenomena persisted also for other forms of nullclines (e.g., an S-shaped one for  $u$  and a sigmoid for  $v$ ) as long as there were the additional two unstable fixed points. Equation (1) actually represents a simplified version of the three-variable reconstruction model for the isothermal CO oxidation on a Pt(110) single-crystal surface [8] which exhibits the same transitions. Experimentally, spiral waves and turbulent patterns in adjacent parameter regions have been observed both in the CO oxidation on Pt(110) [15] and in the NO-NH<sub>3</sub> reaction on Pt(110) [16]. The presented model provides an explanation for these findings.

The results may also be helpful in the context of cardiac arrhythmia, especially the onset of ventricular fibrillation [3,17]. This unfortunate event is preceded by tachycardia, which is attributed to the formation of spiral waves in myocardium [18]. It is still not quite clear how coherence is then destroyed giving rise to fibrillation [18], though turbulence has been reported in a complicated model (Beeler-Reuter) of cardiac activity [19]. On the other hand, in the heart inhomogeneities may play an important role for the formation of noncoherent states, as e.g., in certain results with the Belousov-Zhabotinsky reaction [20]. In contrast, the present system demonstrates an alternative mechanism leading to turbulence due to breakup and subsequent self-replication of spirals in a continuous excitable medium without assuming any inhomogeneities.

The authors are indebted to A. T. Winfree for helpful discussions and for checking the calculations.

- [1] J. J. Tyson and J. P. Keener, *Physica D* **32**, 327 (1988); *Nonlinear Waves in Excitable Media*, edited by A. V. Holden, M. Markus, and H. G. Othmer (Plenum, New York, 1991); *Wave Patterns in Chemical and Biological Systems*, edited by H. L. Swinney and V. I. Krinsky, special issue of *Physica D* **49** (1/2) (1991).
- [2] A. L. Hodgkin and A. F. Huxley, *J. Physiol.* **117**, 500 (1952).
- [3] A. T. Winfree, *When Time Breaks Down* (Princeton University Press, Princeton, 1987).
- [4] G. Gerisch, *Naturwissenschaften* **58**, 430 (1971); P. Devreotes, *Science* **245**, 1045 (1989).
- [5] A. T. Winfree, *Science* **175**, 634 (1972); S. C. Müller, Th. Plesser, and B. Hess, *Science* **230**, 661 (1985).
- [6] A. T. Winfree, *Chaos* **1**, 303 (1991).
- [7] D. Barkley, M. Kness, and L. Tuckerman, *Phys. Rev. A* **42**, 2489 (1990); D. Barkley, *Physica D* **49**, 61 (1991).
- [8] K. Krischer, M. Eiswirth, and G. Ertl, *J. Chem. Phys.* **96**, 9161 (1992); M. Bär, M. Eiswirth, H. H. Rotermund, and G. Ertl, *Phys. Rev. Lett.* **69**, 945 (1992); M. Bär, M. Falcke, and M. Eiswirth, *Physica A* **188**, 78 (1992). In the present paper we made an additional transformation, shifting  $u$  to  $1-u$  and  $v$  to  $1-v$ . Therefore the state  $(u,v)=(0,0)$  corresponds to a CO-covered state.
- [9] M. Gerhardt, H. Schuster, and J. J. Tyson, *Science* **247**, 1563 (1990); H. Ito and L. Glass, *Phys. Rev. Lett.* **66**, 671 (1991).
- [10] A. V. Panfilov and A. V. Holden, *Phys. Lett. A* **151**, 23 (1990).
- [11] G. S. Skinner and H. L. Swinney, *Physica D* **49**, 1 (1991); D. Barkley, *Phys. Rev. Lett.* **68**, 2090 (1992).
- [12] A. Karma, *Phys. Rev. Lett.* **69**, 397 (1992).
- [13] V. Perez-Munuzuri, R. Aliev, B. Vasiev, V. Perez-Villar, and V. I. Krinsky, *Nature* **353**, 740 (1991).
- [14] Y. Kuramoto, *Chemical Oscillations, Waves and Turbulence* (Springer-Verlag, Berlin, 1984); P. Couillet, L. Gil, and J. Lega, *Phys. Rev. Lett.* **62**, 1619 (1989).
- [15] S. Jakubith, H. H. Rotermund, W. Engel, A. von Oertzen, and G. Ertl, *Phys. Rev. Lett.* **65**, 3013 (1990); G. Ertl, *Science* **254**, 1750 (1991).
- [16] G. Vesper, F. Esch, and R. Imbihl, *Catal. Lett.* **13**, 371 (1992).
- [17] A. T. Winfree, *J. Theor. Biol.* **138**, 353 (1989).
- [18] J. M. Davidenko, A. M. Pertsov, R. Salomonsz, W. Baxter, and J. Jalife, *Nature* **353**, 349 (1991).
- [19] M. C. Courtemanche and A. T. Winfree, *Int. J. Bif. Chaos* **1**, 431 (1991).
- [20] K. I. Agladze, V.I. Krinsky, and A. M. Pertsov, *Nature* **308**, 834 (1984).

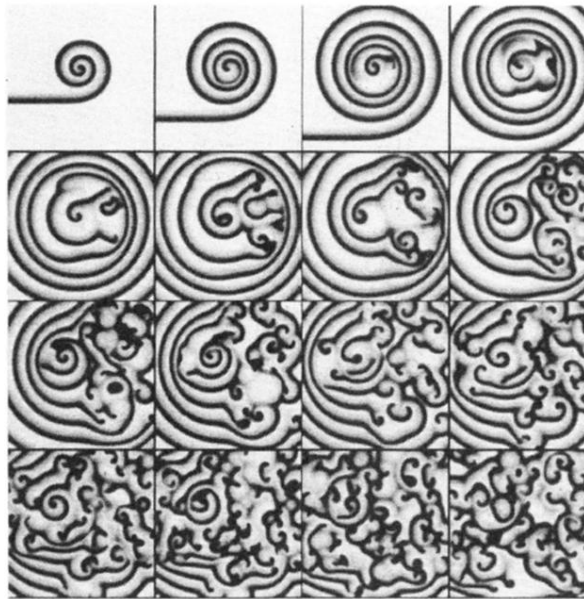


FIG. 2. Development of turbulence at  $a=0.84$ ,  $b=0.07$ ,  $\epsilon=0.08$ . Area of one picture is  $100 \times 100$  (grid points used:  $256 \times 256$ ). Time difference between pictures is 6.41. The initial condition was a flat broken wave. The gray level is proportional to the  $v$  concentration.